Liquid Crystals
Publication details, including instructions for authors and subscription information:
http://www.informaworld.com/smpp/title~content=t713926090

Phase behaviour of thermotropic banana-shaped compounds under pressure

S. Krishna Prasad[a]; Yoji Maeda Corresponding author[a]; D. S. Shankar Rao[b]; S. Anitha Nagamani[b]; Uma S. Hiremath[b]; C. V. Yelamaggad[b]
[a] Nanotechnology Research Institute, National Institute of Advanced Industrial Science and Technology, Tsukuba, Ibaraki 305-8565, Japan [b] Centre for Liquid Crystal Research, Bangalore 560 013, India

Online publication date: 19 May 2010

To cite this Article Prasad, S. Krishna , Maeda Corresponding author, Yoji , Rao, D. S. Shankar , Nagamani, S. Anitha , Hiremath, Uma S. and Yelamaggad, C. V.(2003) 'Phase behaviour of thermotropic banana-shaped compounds under pressure', Liquid Crystals, 30: 11, 1277 — 1283
To link to this Article: DOI: 10.1080/02678290310001610176
URL: http://dx.doi.org/10.1080/02678290310001610176

LIQUID CRYSTALS, VOL. 30, NO. 11, NOVEMBER, 2003, 1277–1283

Taylor & Francis
Taylor & Francis Group

Phase behaviour of thermotropic banana-shaped compounds under pressure

S. KRISHNA PRASAD, YOJI MAEDA*
Nanotechnology Research Institute, National Institute of Advanced Industrial Science and Technology, Higashi 1-1, Tsukuba, Ibaraki 305-8565, Japan

D. S. SHANKAR RAO, S. ANITHA NAGAMANI, UMA S. HIREMATH and C. V. YELAMAGGAD
Centre for Liquid Crystal Research, Jalahalli, Bangalore 560 013, India

(*Received 6 May 2003; accepted 20 June 2003*)

The phase behaviour of two achiral bent core banana-shaped compounds, the hexyloxy (compound I) and decyloxy (compound II) members of the 1,3-phenylene bis[*N*-(2-hydroxy-4-*n*-alkoxybenzylidene)-4′-aminobenzoate] series was investigated under hydrostatic pressures up to 300 MPa using high pressure differential thermal analysis and light transmission methods. The reversible transition sequence crystal (Cr_1)–B_1 phase–isotropic liquid (I), observed at room pressure for compound I, remains in the pressure region up to *c* 70 MPa. At higher pressures a pressure-induced crystalline phase (Cr_i) appears between the Cr_1 and B_1 phases, its temperature region becoming wider with increasing pressure. The temperature vs. pressure phase diagram shows a triple point of 72.9 MPa and 160.3°C for the Cr_1, Cr_i and B_1 phases, indicating the lower limit of pressure for the Cr_i phase. In compound II the reversible transition sequence crystal (Cr_1)–B_2 phase–I is seen over the whole pressure region, and the temperature range of the B_2 phase remains unaltered. It is concluded that both the B_1 and B_2 banana phases are stable over the whole pressure region studied.

1. Introduction

In 1975 Meyer *et al.* [1] showed that tilted smectic liquid crystalline phases of chiral compounds exhibit ferro-, ferri-, and antiferro-electric properties, resulting in the appearance of a macroscopic polarization (**P**). Since then considerable theoretical and experimental studies have been performed on such ferroelectric liquid crystals [2]. Until recently, a prerequisite for the observation of ferroelectricity in liquid crystals was the presence of chiral molecules. A few years ago, however, ferroelectricity was reported in a mesophase, referred to as a B_2 phase, of an achiral system consisting of bent-core, so-called *banana-shaped* molecules [3, 4]. The origin of spontaneous polarization in these systems is believed to be a combination of the following factors. The molecules, having a highly polar character, are arranged in smectic layers in such a way that the dipoles point along a common direction within the layer and are tilted with respect to the layer normal. These factors can give rise to chiral layer symmetry, although the molecules themselves are achiral. Recent investigations have clearly established that the B_2 phase is antiferroelectric [5].

Although numerous experiments have been made on the B_2 phase, there are very few studies on the phase behaviour of banana-shaped compounds under pressure. In fact, there is only a single paper on materials consisting of bent-core molecules [6]. This study involved a compound exhibiting the two-dimensionally ordered B_1 phase, which has been argued to have a columnar structure [7].

In this paper, we present experimental results on the thermal behaviour under pressure of two compounds of the homologous series the 1,3-phenylene bis[*N*-(2-hydroxy-4-*n*-hexyloxy(decyloxy)benzylidene)-4′-aminobenzoate]s, one of which exhibits the B_1 phase (compound I with $n=6$, n being the carbon number in the alkyloxy group) and the other the B_2 phase (compound II, $n=10$). The chemical structure of the compounds I and II are below,

*Author for correspondence; e-mail: yoji.maeda@aist.go.jp

Liquid Crystals ISSN 0267-8292 print/ISSN 1366-5855 online © 2003 Taylor & Francis Ltd
http://www.tandf.co.uk/journals
DOI: 10.1080/02678290310001610176

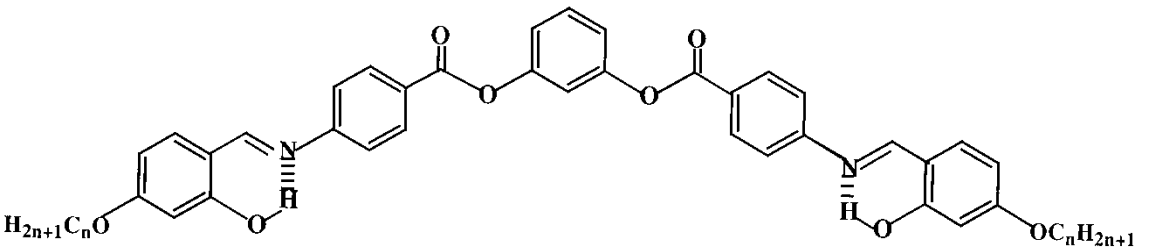

Compound I : $n = 6$
Compound II : $n = 10$

The thermal and optical transmission behaviour of the compounds has been investigated under hydrostatic pressures up to 300 MPa using a high pressure DTA method as well as with a laser transmission technique.

2. Experimental

2.1. *Sample preparation*

The synthesis of compound II is described in our earlier publication [8]; compound I was prepared in a similar way and details will be published elsewhere. Briefly a mixture of 3-(4-aminobenzoyloxy)phenyl 4-aminobenzoate, either 2-hydroxy-4-*n*-hexyloxybenzaldehyde or 2-hydroxy-4-*n*-decyloxybenzaldehyde, absolute ethanol and a trace of acetic acid were heated to reflux until the solid compounds I and II precipitated out, respectively. The crude products obtained were collected by filtration and washed repeatedly with hot ethanol. They were purified by repeated crystallization with a mixture of absolute ethanol/CH_2Cl_2 (9/1) to obtain bright yellow compounds. These were dried under vacuum for 4–5 h and then used for the present studies.

2.2. *Thermal and morphological characterization*

The two compounds were characterized by differential scanning calorimetry (DSC) and polarizing optical microscopy (POM). Thermal characterization was performed on a Perkin-Elmer DSC-7 instrument at a scanning rate of $5^{\circ}C\,min^{-1}$ under N_2 gas flow. Temperatures and heats of transition were calibrated using the standard materials, indium and tin. Transition temperatures were determined as the onset of the transition peaks at which the tangential line of the inflection point of the rising part of the peak crosses the extrapolated baseline. Morphological characterization was performed using a Leitz Orthoplan polarizing optical microscope equipped with a Mettler hot stage FP-82.

2.3. *Optical measurements under pressure*

The details of the optical high pressure cell have been described in an earlier paper [9]. Essentially it consists of a sample sandwiched between two optically polished sapphire rods enclosed in an elastomeric tube. Low viscosity oil was used as the pressurizing medium. The light intensity of a He-Ne laser beam transmitted through the sample was monitored as a function of temperature using a photodiode with a built-in amplifier. The experiments were performed under isobaric conditions, i.e. the temperature was varied at a controlled rate of $\sim 1^{\circ}C\,min^{-1}$ under a constant pressure. Pressure was measured to a precision of 1.5 bar using a Heise gauge. A PC handled the data acquisition and control of the experiment.

2.4. *DTA measurements under pressure*

The high pressure DTA apparatus used in this study is described elsewhere [10]. The DTA system was operated in a temperature region between room temperature and 250°C under hydrostatic pressures up to 300 MPa. Dimethylsilicone oil with a medium viscosity (100 cSt) was used as the pressurizing medium. The sample weighing about 4 mg was put in the sample cell and coated with epoxy adhesives, to fix the sample in the cell and also to prevent direct contact with the silicone oil. The DTA runs were performed at a constant scanning rate of $5^{\circ}C\,min^{-1}$ under various pressures. Transition temperatures were determined in the same manner as in the DSC analysis. Transition enthalpies under pressure were estimated using the general procedure for estimation of transition enthalpy based on heat-flux DSC. For the purpose of calibration the enthalpy of fusion for indium was measured at various pressures, and then a calibration curve for the standard value ΔH of indium was constructed and the apparatus constants were determined as a function of pressure. Since the compounds are not very stable, a new sample was used for each DTA measurement.

3. Results and discussion

3.1. *Characterization under atmospheric pressure*

Figure 1 shows the DSC curves of compounds I and II. Compound I shows the reversible transition sequence $Cr_1 \leftrightarrow B_1 \leftrightarrow I$. In the case of compound II the pure (solvent-crystallized) sample shows three peaks in

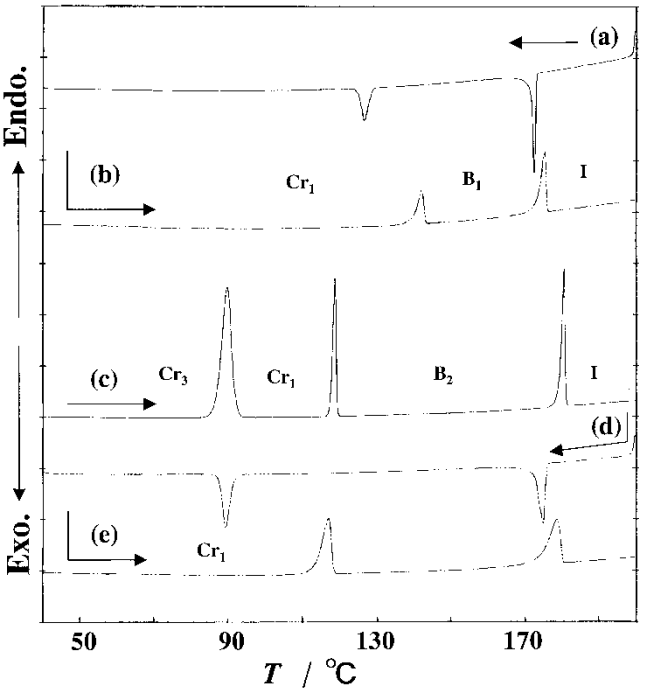

Figure 1. DSC curves of compounds I and II at a scanning rate of 5°C min^{-1}: (*a*) cooling and (*b*) heating runs for compound I; (*c*) heating run of pure compound II; (*d*) and (*e*) first cooling and subsequent heating runs for compound II.

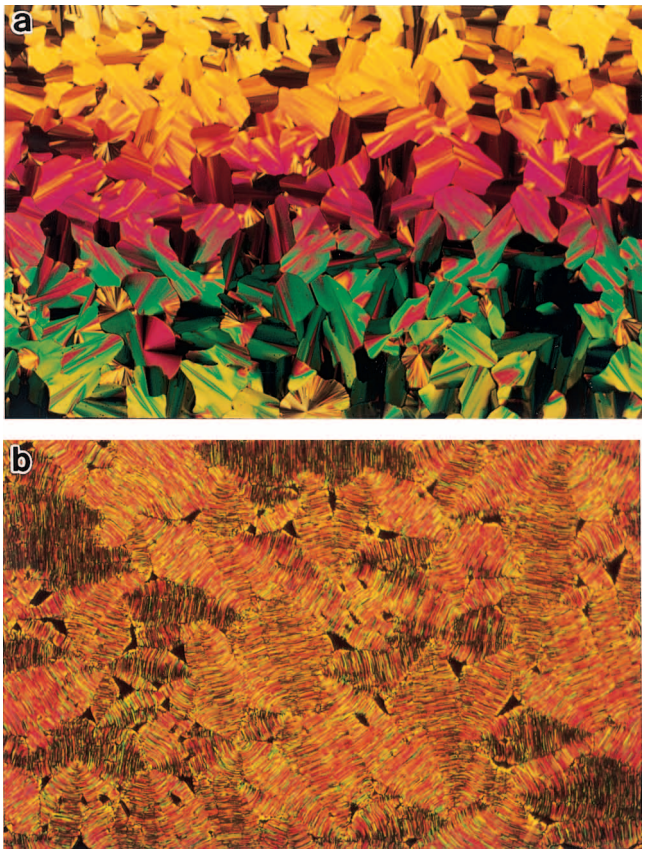

Figure 2. POM photographs of textures of (*a*) B_1 phase observed at 161°C for compound I, and (*b*) B_2 phase observed at 146°C for compound II.

the first heating run, which are identified as low to high temperature crystal transition (Cr_3–Cr_1), melting (Cr_1–B_2) and clearing (B_2–I) transitions. The cooling and subsequent heating runs (melt-crystallized sample) show only two peaks corresponding to the Cr_1–B_2 and B_2–I transitions. Since the low to high temperature crystal transition splits into a doublet under pressure as described in the later sections, the first transition of the pure sample seems to be composed of the Cr_3–Cr_2 and Cr_2–Cr_1 transitions, but these crystalline phases appear neither on cooling from the isotropic liquid nor in subsequent heating runs.

The B_2 phase of this compound is identified using electro-optic switching and X-ray studies [8]. The thermodynamic quantities associated with the phase transitions for the two compounds are listed in the table. An attractive feature of these compounds over other bent-core molecules is a large temperature range for the mesophases, ~35°C and ~57°C for the B_1 and B_2 phases, respectively.

Figure 2 shows POM photographs of textures observed for the B_1 (*a*) and B_2 (*b*) phases of compounds I and II, respectively. The B_1 phase of compound I exhibits a typical mosaic texture, while the B_2 phase of compound II shows many spherulitic domains with a fringe pattern superimposed on a focal-conic texture.

Table. Thermodynamic quantities associated with the phase transitions obtained in the heating mode for compounds I and II.

	T/°C	ΔH/kJ mol^{-1}	ΔS/J K^{-1} mol^{-1}	dT/dP/K MPa^{-1}	ΔV^a/cm^3 mol^{-1}
Compound I (n=6)					
Cr_1–B_1	143.4	37.2	89.3	0.175_6	15.7
B_1–I	175.3	16.7	37.2	0.280_4	10.4
Compound II (n=10)					
Cr_3–Cr_1	86.0	52.0	144.8	0.214_4	31.0
Cr_1–B_2	117.5	22.7	58.2	0.289_5	16.8
B_2–I	180.0	24.5	54.1	0.298_7	16.2

[a]Transition volume calculated using the Clausius–Clapeyron equation.

3.2. *Phase behaviour of compound I under pressure*

Figure 3 shows the DTA heating curves of compound I at various pressures. The heating curves at 20 and 40 MPa show the strong peak of the Cr_1–B_1 transition and a relatively broad peak for the B_1–I transition at higher temperatures. The Cr_1–B_1–I transition sequence, observed at atmospheric pressure, is seen also in the lower pressure range. Increasing the pressure above ~100 MPa, however, induces a crystal phase (Cr_i) between the Cr_1 and B_1 phases. The heating curves show that at higher pressures the strength of the $Cr_i \rightarrow B_1$ peak increases at the expense of the Cr_1–Cr_i peak. The $B_1 \rightarrow I$ transition peak is quite small at high pressures. Thus in the high pressure region the Cr_1–Cr_i–B_1–I transition sequence is observed. Figure 4 shows the *T*–*P* phase diagram of compound I at pressures up to 300 MPa. All of the phase transition curves can be described by a linear function of pressure as follows:

$$0 < P < 70\ \text{MPa}$$

$$Cr_1 \rightarrow B_1 \qquad T/^\circ\text{C} = 142.4 + 0.245_3\ P/\text{MPa}$$

$$70\ \text{MPa} < P$$

$$Cr_1 \rightarrow Cr_i \qquad T/^\circ\text{C} = 154.1 + 0.084_3\ P/\text{MPa}$$

$$Cr_i \rightarrow B_1 \qquad T/^\circ\text{C} = 142.4 + 0.245_3\ P/\text{MPa}$$

whole pressure range

$$B_1 \rightarrow I \qquad T/^\circ\text{C} = 177.2 + 0.289_1\ P/\text{MPa}$$

The melting line (Cr_1–B_1 at low pressures and $Cr_i \rightarrow B_1$ at high pressures) and the Cr_1–Cr_i line intersect at an intermediate pressure, resulting in a triple point for the Cr_1, Cr_i, and B_1 phases. The triple point was determined as 72.9 MPa, 160.3°C, which is the lower limit of pressure for the Cr_i phase. Interestingly the temperature range for the B_1 phase remains almost unchanged at about 35°C in the whole pressure range up to 300 MPa. Weissflog *et al.* [6] reported similar thermal behaviour for the B_1 phase of the *N*,*N*′-bis[4-(4-*n*-octyloxybenzoyloxy)benzylidene]phenylene-1,3-diamines and obtained an interesting temperature vs. pressure phase diagram. At higher pressures two transition peaks appear reversibly below the clearing point. A new stable high pressure phase, denoted as Cr_2, is clearly seen. They also determined a triple point (84 MPa, 135°C) for the Cr_1, Cr_2, and B_1 phases, indicating the lower limit of the high pressure Cr_2 phase. It is interesting to see that a pressure-induced crystalline phase is formed for both compounds showing the B_1 phase.

Figure 5 shows (for compound I) the pressure dependence of the transition enthalpies for the Cr_1–B_1 transition in the low pressure region, the Cr_1–Cr_i and Cr_i–B_1 transitions in the high-pressure region, and for the B_1–I transition in the whole pressure region, that have been qualitatively estimated. The enthalpy for the Cr_1–B_1 transition is relatively high in the low pressure region below 60 MPa. In the high pressure region, however, the enthalpy for the Cr_1–Cr_i transition becomes smaller with increasing pressure, while the Cr_i–B_1 transition is increased. On the other hand, the enthalpy for the B_1–I transition decreases marginally with pressure.

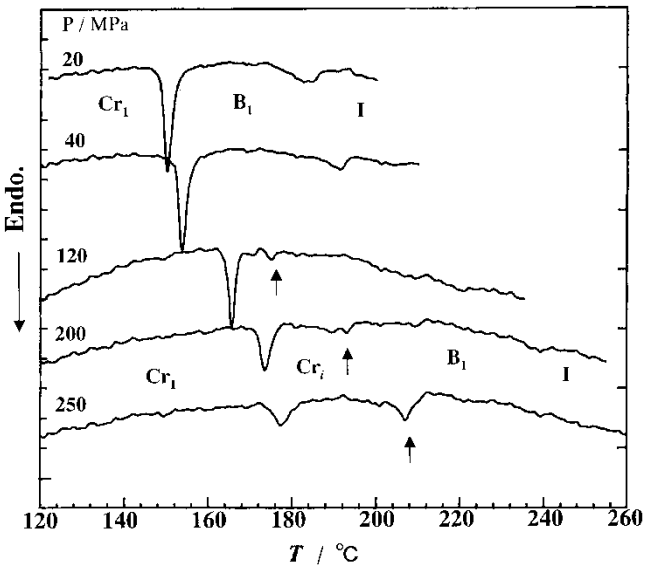

Figure 3. DTA heating curves of compound I at various pressures; heating rate 5°C min^{-1}. The arrows indicate the transition to the B_1 phase from the pressure-induced Cr_i phase.

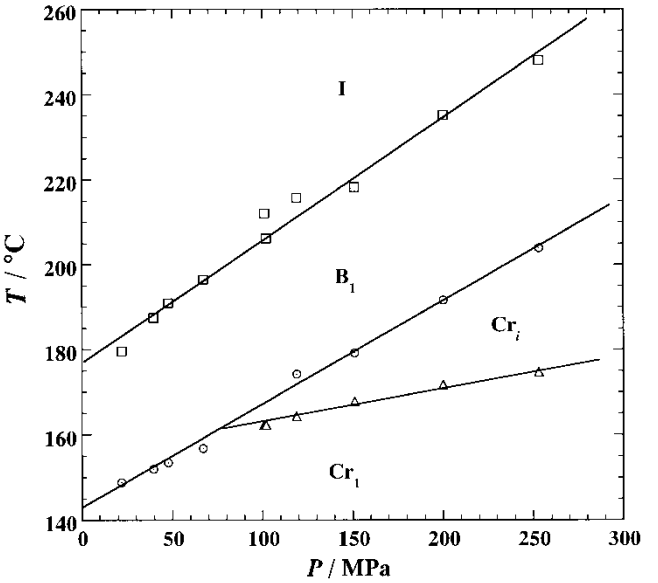

Figure 4. *T* vs. *P* phase diagram for compound I. Note that the temperature range of the B_1 phase is essentially the same over the entire pressure range and that a crystalline phase (Cr_i) is induced at high pressures.

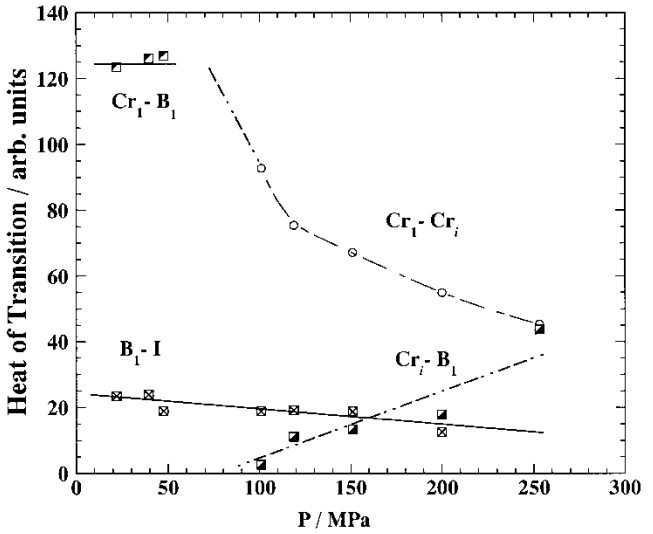

Figure 5. Plots showing the pressure dependence of the transition enthalpies of the various transitions for compound I.

3.3. *Phase behaviour of compound II under pressure*

Figure 6 shows the heating curves of pure samples of compound II at 100 and 200 MPa. The first heating runs of the pure samples show the same behaviour as one at atmospheric pressure, except that the first peak exhibits a shoulder. Thus the first endothermic peak indicates the occurrence of consecutive crystal transitions, i.e the Cr_3–Cr_2 followed by the Cr_2–Cr_1 transition under pressure. Figure 7 shows the second heating curves of compound II at various pressures.

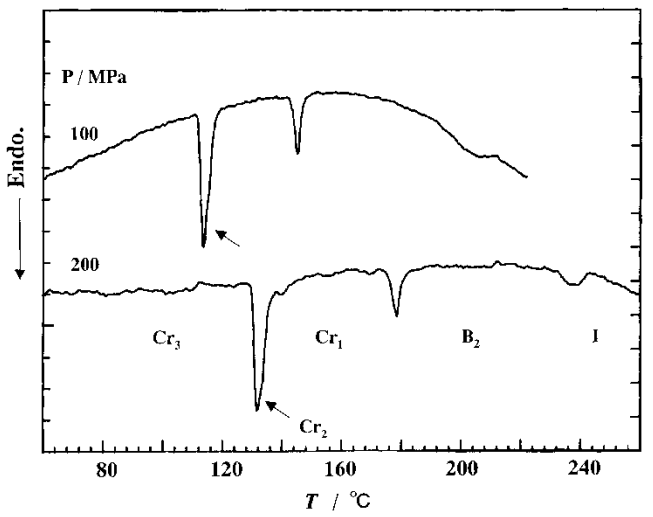

Figure 6. DTA heating curves of pure compound II at 100 and 200 MPa; heating rate 5°C min^{-1}. The arrows indicate the region of the Cr_2 phase.

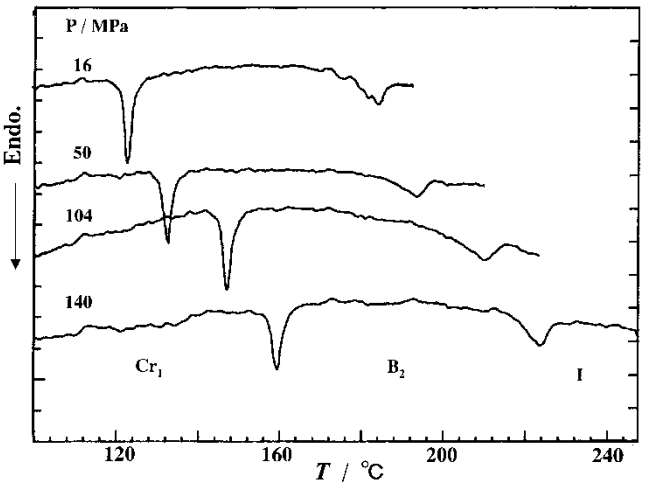

Figure 7. Second heating curves of compound II at various pressures.

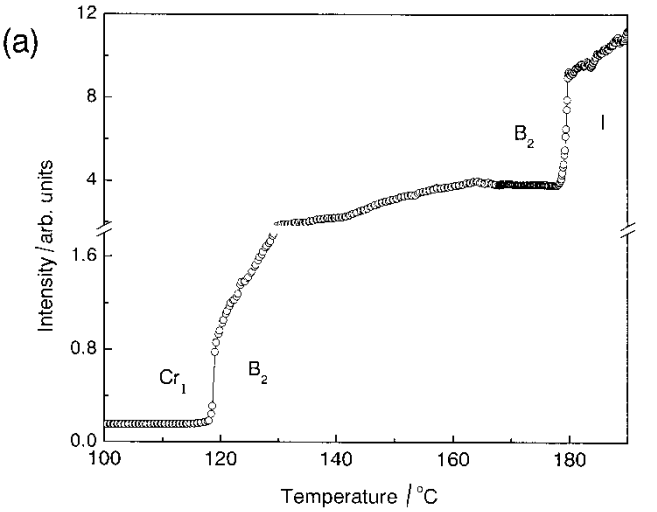

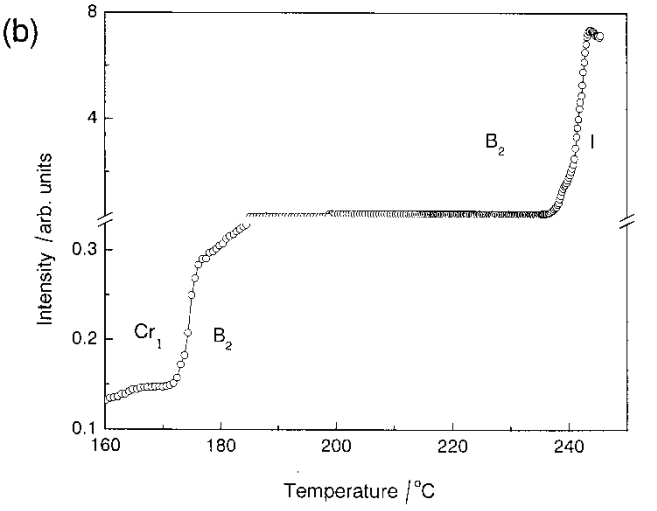

Figure 8. Laser transmission intensity as a function of temperature for compound II recorded on heating at (*a*) atmospheric pressure and (*b*) 191 MPa.

The second runs under pressures show only the Cr_1–B_2–I transition sequence in the whole pressure region. Accordingly the Cr_3 and Cr_2 crystalline phases in the pure sample show monotropic transition behaviour under hydrostatic pressure.

Figures 8 (*a*) and 8 (*b*) show the raw data of the transmitted light intensity vs. temperature experiments for compound II at atmospheric pressure and 191 MPa, respectively. The onset of the phase transition is marked by an abrupt variation in the intensity, and the temperature corresponding to the mid-point of the intensity jump was taken to be the transition temperature. The salient feature to be noted is that the temperature range of the B_2 phase remains unaltered between the two pressures.

Both pressure vs. temperature phase diagrams obtained from optical and DTA measurements are shown in figure 9. It can be seen that both the Cr_1 and B_2 phases are stable in the whole pressure region studied. The temperature range of the B_2 phase remains almost the same ($\sim$57°C) over the entire range of pressures because the melting and clearing point transition lines run parallel to each other. This feature is also seen for compound I in which the temperature range of the B_1 phase remains unaltered ($\sim$35°C) with pressure. The transition curves in figure 9 can be described by linear functions in pressure over the whole pressure range investigated, as thus,

Cr_3–Cr_2	$T/°C = 89.6 + 0.211_0\ P/MPa$
Cr_2–Cr_1	$T/°C = 92.7 + 0.201_0\ P/MPa$
Cr_1–B_2	$T/°C = 116.8 + 0.293_4\ P/MPa$
B_2–I	$T/°C = 173.9 + 0.288_6\ P/MPa$

The pressure independence of the temperature range of a mesophase (in this case the B_2 phase) is not uncommon in liquid crystalline systems. Even the dT/dP ratios of 0.293°C MPa^{-1} for the Cr_1–B_2 and 0.288°C MPa^{-1} for the B_2–I transitions are comparable to some of the results reported earlier for transitions involving the smectic A phase [9]. Figure 10 shows the pressure dependence of the transition enthalpies and entropies for the Cr_3–(Cr_2)–Cr_1, Cr_1–B_2 and B_2–I transitions of compound II. The associated transition enthalpies of 23.0 and 14.0 kJ mol^{-1} for the Cr_1–B_2 and B_2–I transitions, respectively, are relatively large. As Weissflog *et al* [6] discussed, the thermodynamic quantities for the Cr_1–B_1 and B_1–I transitions based on the Clausius–Clapeyron equation (the ΔH and ΔV

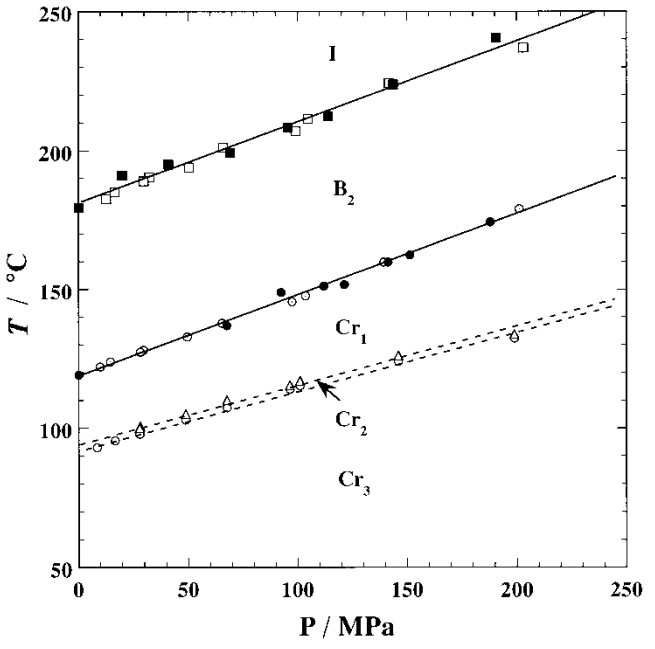

Figure 9. *T* vs. *P* phase diagram of compound II constructed from the data obtained by optical (filled symbols) and DTA (open symbols) measurements.

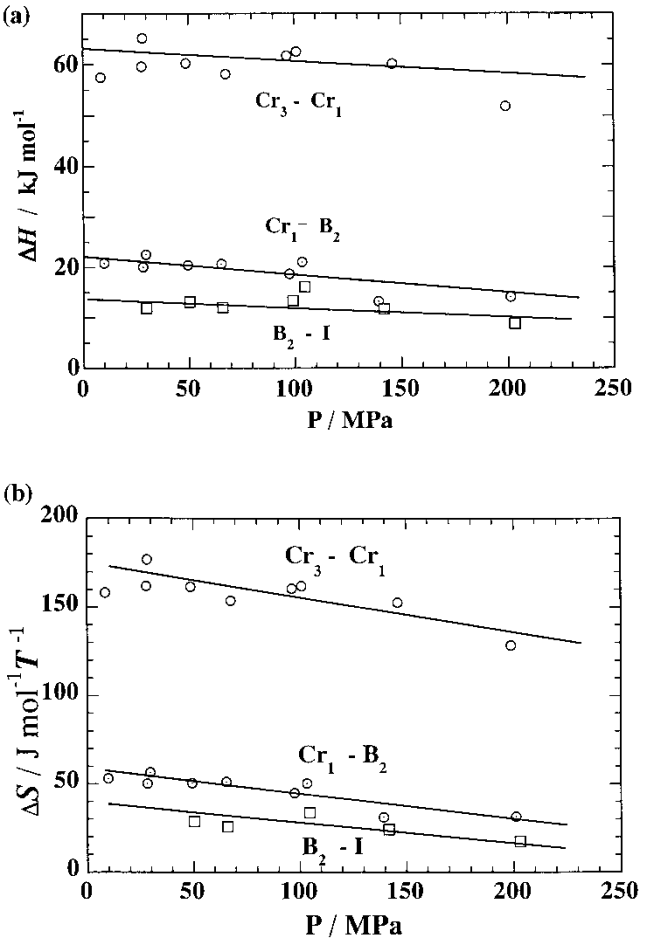

Figure 10. The dependence of (*a*) transition enthalpies and (*b*) entropies on pressure for compound II.

values associated with the Cr–B_1 and B_1–I transitions) for compound I are not very different (see the table), indicating the relatively high degree of order in the B_1 phases. Furthermore it can be seen that the same relationship exists in the B_2 phase of compound II.

In this study the phase transition behaviour of two banana-shaped bent-core compounds has been investigated under hydrostatic pressures up to 300 MPa using optical and DTA methods. From the experimental results it is concluded that both the B_1 and B_2 banana phases are stable in the whole pressure region studied.

S.K.P thanks the Japan Society for Promotion of Science for an invitation fellowship during the course of this work.

References

[1] MEYER, R. B., LIEBERT, L., STRZELECKI, L., and KELLER, P., 1975, *J. Phys. (Paris)*, **36,** L69.

[2] For example, see Lagerwall, S. T., 1999, *Ferroelectric and Antiferroelectric Liquid Crystals*, (Weinheim: Wiley-VCH).

[3] NIORI, T., SEKINE, T., WATANABE, J., FURUKAWA, T., and TAKEZOE, H., 1996, *J. mater. Chem.*, **6,** 1231.

[4] PELZL, G., DIELE, S., and WEISSFLOG, W., 1999, *Adv. Mater.*, **11,** 707.

[5] WALBA, D. M., KORBLOVA, E., SHAO, R., MACLENNAN, J. E., LINK, D. R., GLASER, M. A., and CLARK, N. A., 2000, *Science*, **288,** 2181.

[6] WEISSFLOG, W., WIRTH, I., DIELE, S., PELZL, G., SCHMALFUSS, H., SCHOSS, T., and WÜRFLINGER, A., 2001, *Liq. Cryst.*, **28,** 1603.

[7] SHEN, D., PEGENAU, A., DIELE, S., WIRTH, I., and TSCHIERSKE, C., 2000, *J. Am. chem. Soc.*, **122,** 1593.

[8] YELAMAGGAD, C. V., HIREMATH, U. S., ANITHA NAGAMANI, S., SHANKAR RAO, D. S., and KRISHNA PRASAD, S., 2001, *J. mater. Chem.*, **11,** 1818.

[9] SHANKAR RAO, D. S., VIVEK KUMAR, G., KRISHNA PRASAD, S., MANICKAM, M., and KUMAR, S., 1998, *Mol. Cryst. liq. Cryst.*, **319,** 193.

[10] MAEDA, Y., and KANETSUNA, H., 1985, *Bull. Res. Inst. Polym. Tex.*, **149,** 119; Maeda, Y., 1990, *Thermochim. Acta*, **163,** 211.